Int. J. Multiphase Flow Vol. 18, No. 3, pp. 423–437, 1992
Printed in Great Britain.

0301-9322/92 $5.00 + 0.00

THE DEVELOPMENT OF A FLUSH-WIRE PROBE AND CALIBRATION METHOD FOR MEASURING LIQUID FILM THICKNESS

H. C. KANG and M. H. KIM
Department of Mechanical Engineering, Pohang Institute of Science and Technology, P.O. Box 125, Pohang 790-600, South Korea

(Received 19 March 1991; in revised form 17 December 1991)

Abstract— A new conductance probe, referred to as a flush-wire probe, is proposed to enhance the spatial resolution for the continuous measurement of liquid film thicknesses. Its spatial resolution is compared with that of typical conductance probes numerically and experimentally. A new calibration technique using the probability of the the liquid's existence at several liquid film heights is also proposed, and shown to be more accurate and stable than previous methods.

Key Words: liquid films, measurement, calibration method, conductance probe

1. INTRODUCTION

The wavy liquid film encountered in various two-phase flow systems has a major influence on the heat and mass transfer characteristics of these systems. Instantaneous measurement of the film thicknesses is very useful in understanding these characteristics in a stratified flow.

Hitherto, a large number of experimental techniques have been used to measure the exact liquid film thickness and have been partially successful. For very thin (0.1–4 mm) and fast fluctuating (up to hundreds of hertz) films, traditional techniques are insufficient for the accurate measurement of time-varying thin liquid film thicknesses. Initially, the liquid wave forms were examined with the naked eye or by simple devices. Neal & Bankoff (1963) and numerous researchers measured liquid film thickness using a needle-contact probe. This probe is accurate and easy to handle, but gives limited data about the existence of the liquid at the probe location. Salazar & Marschall (1978) and Akai *et al.* (1980) measured the interface characteristics using laser scattering and hot film probes, but these did not easily yield the absolute film height. In spite of difficulties in data reduction, conductance probes using the electrical conductivity of liquids have been widely used to obtain continuous measurements of liquid film thicknesses since the 1960s. A number of electrode geometries have been utilized. Collier & Hewitt (1964) and numerous investigators have used flush-mounted probes consisting of two electrodes placed on the surface under the the film. Coney (1973) mentioned that the flush-mounted probe had reasonable thickness resolution for measurements in thin liquid films (<2 mm). However, the resolution decreased for thicker films. With the development of parallel-wire probes immersed in the liquid, it was possible to increase the range of film thickness over which the instrument was useful. This type of probe may have been used first by Swanson (1966) and later by Miya *et al.* (1971). Brown *et al.* (1978) estimated theoretically the response of the parallel-wire probe for a two-dimensional square wave disturbance in a film. They remarked that the ratio of the inner-wire distance to the wire size is important in decreasing the damping effect of the probe. Koskie *et al.* (1989) presented more clearly an arrangement of the wire probes that increased the spatial resolution obtained by calculation of the resistance between the electrodes, but the resulting probes yielded some error for thin liquid films (<1 mm).

Calibration methods have varied with different researchers. Chu & Dukler (1974) calibrated their probe using annular gaps which were formed between the outer wall and a series of inserts of diameter smaller than the outer wall. Karapantsios *et al.* (1989) and other researchers carried out the calibration outside the test section without consideration of the actual probe mounted in the test section. It was known that the parallel-wire probe gives a linear response to film thickness.

However, Koskie *et al.* (1989) mentioned that calibration of the parallel-wire probe was necessary to determine the effect of actual probe geometry, and that nonlinearity was probably due to a combination of nonparallel wires and electrical resistance in wires and leads. Thus, spatial resolution and calibration have been typical problems in the practical use of the conductance probe.

In this paper, a new type of conductance probe, hereafter referred to as a flush-wire probe, is proposed to enhance the spatial resolution. The spatial resolution of the flush-wire probe is proved numerically and experimentally to be better than that of the other conductance probes. Also, a new calibration technique using the probabilities of the liquid's existence at various film heights is presented.

2. SPATIAL RESOLUTION

Conductance probes have been widely used to measure the instantaneous liquid film thickness using a relationship between the film thickness and the electrical resistance of the liquid. Typical conductance probes are classified into two types, such as the parallel-wire probe and the flush-mounted probe shown in figures 1(b) and 1(c), respectively. The newly developed flush-wire probe consists of an electrode which is flush with the wall and a wire electrode which is vertically inserted from the top side, as shown in figure 1(a).

The admittance of the electrolyte is a function of input frequency. Brown *et al.* (1978) mentioned that the phase of the admittance of the electrolyte, such as water, reaches zero when the frequency of the input signal is above 100 kHz (figure 2 of their paper). At these high frequencies, the only equivalent component which remains in the electrolyte is resistance. These facts are reconfirmed by an RLC meter (Hewlett Packard model 4274A) for the three types of conductance probe in this work. The size of an electrolyte region (a few millimeters) for which the variation of electric potential is negligible is very small in comparison with the wavelength (up to several hundred meters) of an oscillating electromagnetic field. For the region, the electromagnetic field can be approximated as a time invariant. The governing equation for the electrolyte is

$$\nabla^2\phi = -4\pi\rho, \qquad [1]$$

where ϕ and ρ are the electrical potential and charge density, respectively. Because no charge source exists at the electrolyte, [1] reduces to the Laplace equation

$$\nabla^2\phi = 0. \qquad [2]$$

Since the interface and the plate which is covered with the liquid film are very electrically resistive, the boundary conditions for all interfaces can be assumed to be

$$\frac{\partial\phi}{\partial n} = 0. \qquad [3]$$

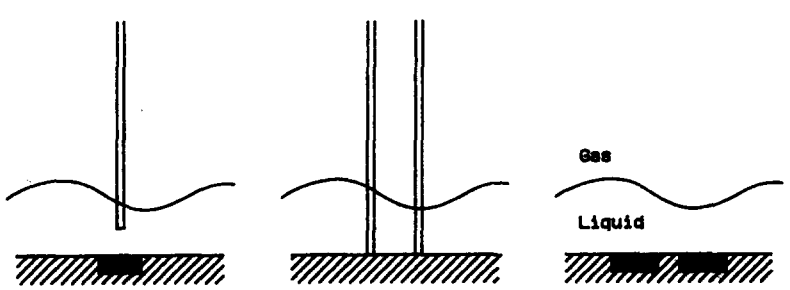

(a) Flush-Wire Probe (b) Parallel-Wire Probe (c) Flush-Mounted Probe

Figure 1. Schematic diagram of the conductance probes.

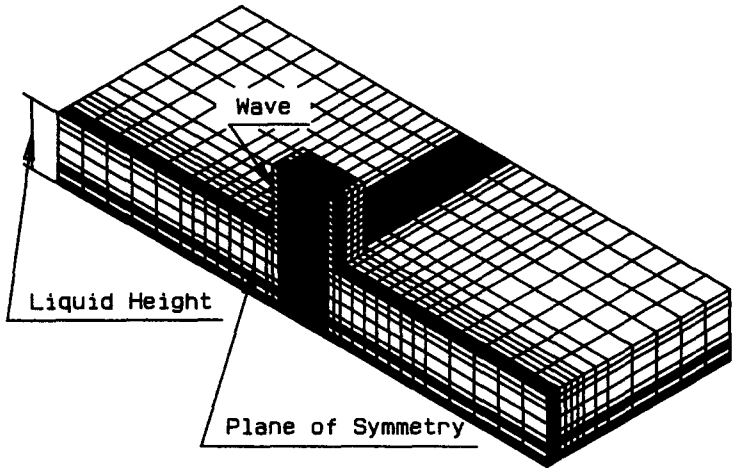

Figure 2. Three-dimensional grids for the numerical analysis.

As the two electrodes of a conductance probe are usually made of low-resistivity metals such as platinum, the electric potential can be assumed to be equal within them. The boundary conditions for the electrodes can be written as follows:

$$\left.\begin{array}{ll} \phi = V & \text{at the source electrode} \\ \phi = 0 & \text{at the measuring electrode.} \end{array}\right\} \quad [4]$$

Assuming the electrical conductivity of the electrolyte to be constant and uniform, the current between I between two electrodes can be written using electromagnetic theory as

$$I = \frac{\sigma}{V} \int_{\upsilon} |\nabla \phi|^2 \, d\upsilon, \quad [5]$$

where σ, V and υ are the electric conductivity of the liquid, the potential difference between the electrodes and the calculation domain, respectively.

The ideal conductance probe would output a current related only to the liquid film height at the probe location, with no effect from other waves. The signal output is, however, affected by the waves around the conductance probe. To examine the wave effect, a moving cubic wave of side length 1 mm is assumed on the constant liquid film of 1 mm thickness. In the rough calculation, the length where the electrical potential is affected is a few millimeters. Therefore, the base calculation domain in modeling the thin liquid film is taken as 1 mm high, 3 mm wide and 8 mm long in the numerical analysis. The numbers of grid steps in the length, width and height directions of the base calculation domain are 45, 21 and 19, respectively, as shown in figure 2. The analysis models of the conductance probe are shown in figure 3. These geometries are taken from the shapes

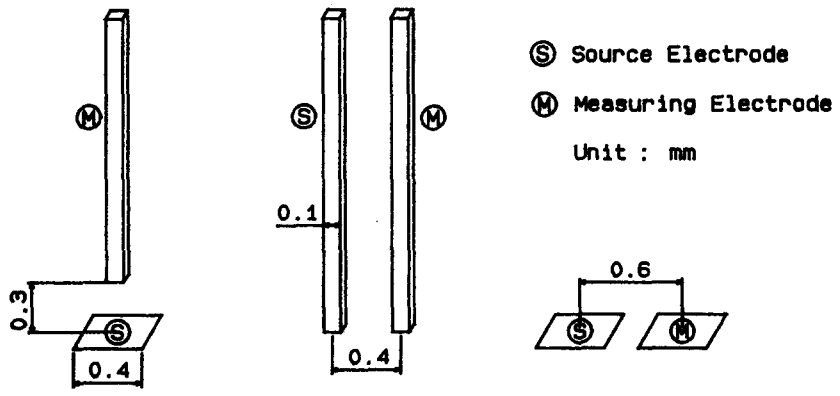

Figure 3. Conductance probe geometries for numerical analysis.

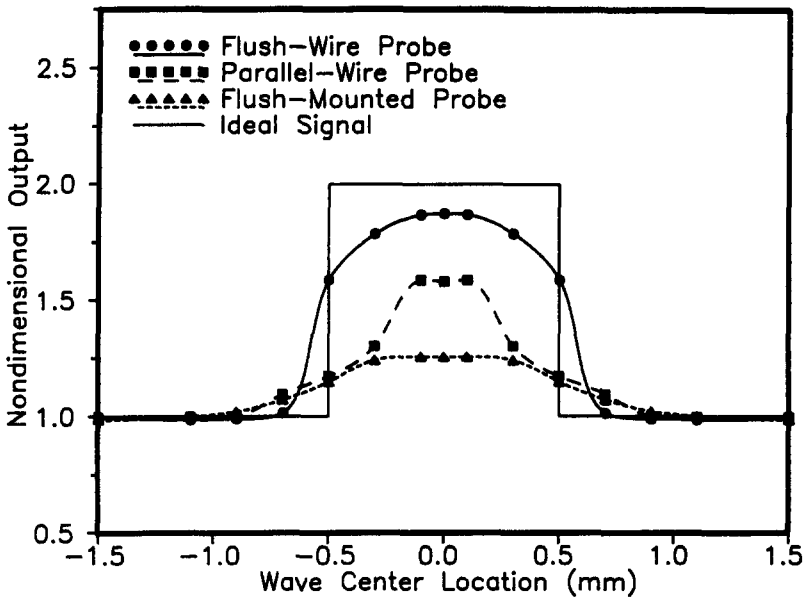

Figure 4. Nondimensional outputs with the ideal square wave vs wave center locations.

of Koskie *et al.* (1989) and Collier & Hewitt (1964). The governing equation [2], is solved using a three-dimensional finite difference method to obtain the electrical potential with boundary conditions [3] and [4]. The total current output between the electrodes is calculated using [5] at eight locations of the wave center, apart from the conductance probes which are fixed at the center of the calculation domain. In comparison with the spatial resolution of the conductance probes, the output of the conductance probe with a cubic wave is nondimensionalized by that of the flat liquid without waves as follows:

$$I^* = \frac{I_{mw}}{I_{nw}} = \frac{\left(\int_v |\nabla\phi|^2 \, dv\right)_{mw}}{\left(\int_v |\nabla\phi|^2 \, dv\right)_{nw}}, \qquad [6]$$

where subscripts "nw" and "mw" mean without and with waves, respectively.

The nondimensional output (I^*) for the conductance probes of figure 3 is shown in figure 4. The ideal output should be a rectangular wave (the solid line in figure 4), but some damping of this form can be expected in the measurement. The output of the parallel-wire probe is closer to the ideal signal than that of the flush-mounted probe, in agreement with previous research. But the spatial resolution of the flush-wire probe is better than that of the other two probe types.

The spatial resolution of the flush-wire probe depends on the dimensions of the flush-wire probe, such as the diameter (d), the flush-probe diameter (D), water film thickness (h) and immersed length (l). Further numerical analysis was done to search for the best geometric condition of the flush-wire probe. Another nondimensional output (I^+) is defined by the current through the liquid region of radius r divided by the current through the total liquid region, as follows:

$$I^+ = \frac{I_r}{I_t} = \frac{\left(\int_v |\nabla\phi|^2 \, dv\right)_r}{\left(\int_v |\nabla\phi|^2 \, dv\right)_t}. \qquad [7]$$

Equation [7] is calculated in the same way as [6], by the finite difference method in cylindrical coordinates.

The liquid column diameter where the output (I_r) reaches 99% of the total output (I_t) is defined as the critical diameter (D_{sp}). The spatial resolution is improved by decreasing the critical diameter, since most of the current passes through this critical region. For a wire diameter of 0.075 mm and

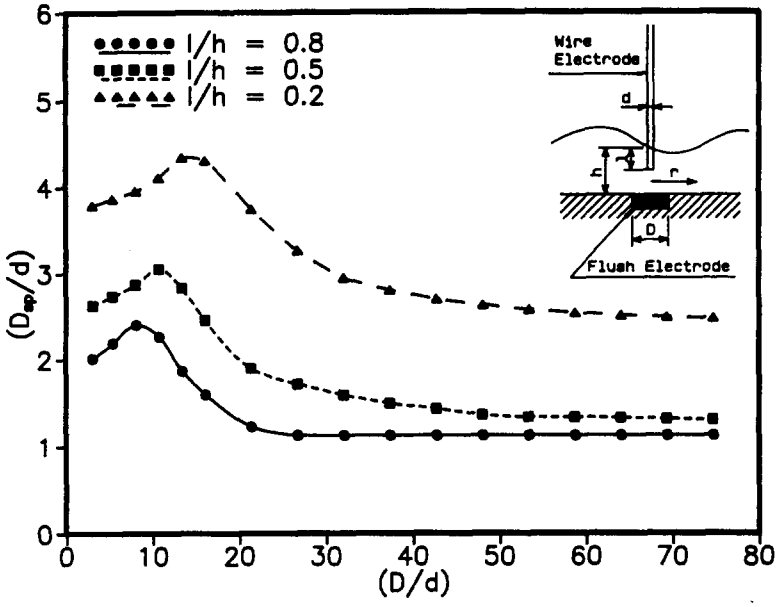

Figure 5. 99% Concentration regions ($h/d = 28.6$).

a moderate 2 mm film height, the critical diameter is calculated as shown in figure 5. This figure shows that the critical diameters decrease with increasing diameter ratio (D/d) and immersed length ratio (l/h). The critical diameters are only 1.13–4.3 times the wire diameter (d) along the diameter ratio (D/d) and the immersed length ratio (l/h). Since a large immersed depth ratio gives better spatial resolution, the resolution is better at the wave crest than at the wave trough. It is recommended that the wire probe is immersed further than half of the minimum film thickness. Figure 6 shows the variation of the nondimensional output (I^+) with increasing diameter of the liquid column. This figure clearly shows that most of the current passes within only twice the wire diameter. In conclusion, it is clear that the spatial resolution can be enhanced up to the order of the wire diameter in the flush-wire probe.

Koskie *et al.* (1989) remarked that 99% of the resistance concentration region of their parallel-wire probe is more than 20 times the wire diameter. Since the immersed length ratio (l/h) is changeable, the spatial resolution of a flush-wire probe can be improved to <0.1 mm using a

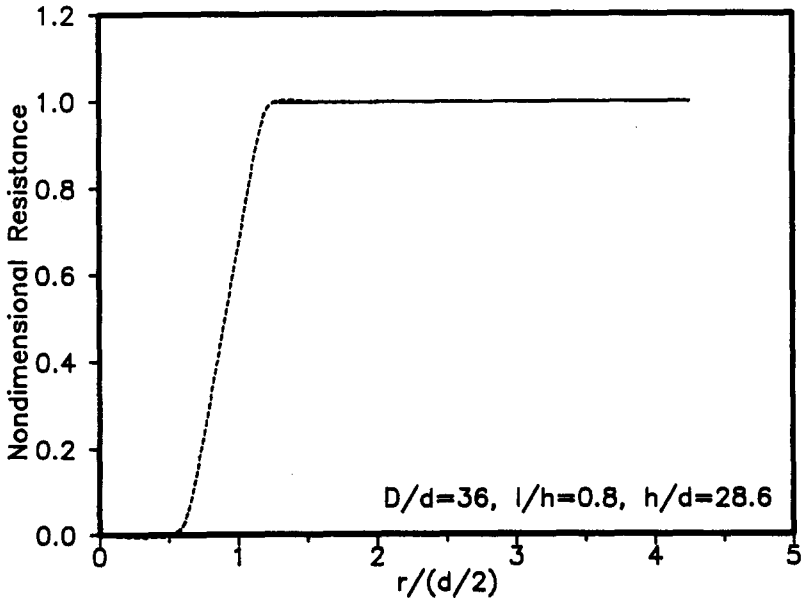

Figure 6. Variation of nondimensional resistance along the radius of the liquid column.

flush-wire probe with a large flush electrode ($D/d > 30$) and immersed depth ratio ($l/h > 0.5$). Since the wavelength is larger than a few millimeters in a moderate air–water stratified flow, the newly developed flush-wire probe can measure wavy film thickness at the probe location alone, with no effect from other waves.

3. CALIBRATION METHOD

The electrical conductivity of the liquid has been used for the calibration of conductance probes in previous works. In real measurements, it is very difficult to maintain the liquid and probes in the same condition as in the calibration. The conductivity of the liquid is a strong function of temperature and contaminants etc. A compensation circuit and reference probe have been used to avoid these effects in previous works (Chu & Dukler 1974; Koskie *et al.* 1989). But the status of the probe is very sensitive to environmental conditions, such as contaminants, bubbles and dust on the electrode. The condition of probes such as a hot-wire probe is very difficult to control.

The probability of the liquid's existence at any height, however, is unique when the liquid flow rate is constant. The probabilities of the liquid's existence change monotonically with the liquid heights, and can easily be measured by the well-known needle-contact probe. Calibration using probability is a very powerful tool for the conductance probe. Figure 7 shows the concept of calibration using probabilities.

The contact probability of the liquid, i.e. the probability of the liquid's existence at any height h_i, is given by

$$Pn_i = f_1(h_i) = \frac{t_n}{t_t}, \qquad [8]$$

where Pn_i is the contact probability of the needle-contact probe at the height h_i, and t_t and t_n are the total measuring time and the sum of contact times of the needle-contact probe with the liquid, respectively. The subscript "i" denotes the different locations of the needle-contact probe. The output of the conductance probe at any liquid film height h_i is given by

$$Vc_i = f_2(\sigma, s, h_i), \qquad [9]$$

where σ and s are the conductivity of the liquid and the status of the probe. If it takes a short time to measure the output voltages of the conductance probe by the data acquisition system, the electric

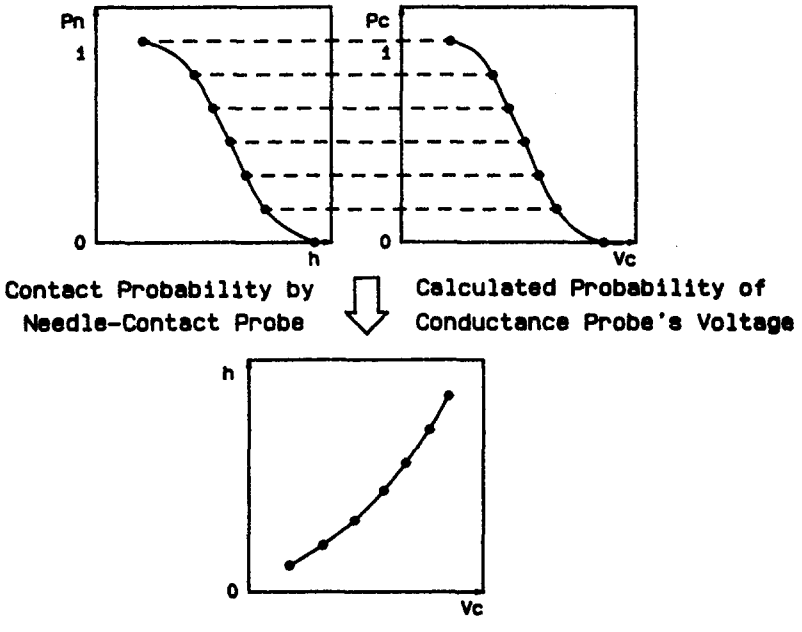

Figure 7. Concept of the calibration method using probabilities.

conductivity (σ) and the status of the probe (s) during this period can be assumed to be constant. If the conductance probe has good spatial resolution, the output voltage Vc_i only depends on the film height and can be expressed as follows:

$$Vc_i = f_3(h_i). \quad [10]$$

If the wave form is not a folding wave, the output Vc_i of the conductance probe changes monotonically with the film height. The probability Pc_i of the conductance being larger than any voltage Vc_i at the film height, h_i is expressed as

$$Pc_i = f_4(Vc_i) = \frac{t_c}{t_t}, \quad [11]$$

where t_t and t_c are the total time and the sum of times above Vc_i, respectively. At any film height h_i, the probabilities of Pn_i and Pc_i must be equal. The calibration curves, i.e. the relationship between h_i and Vc_i, can be obtained from the probabilities of Pn_i and Pc_i in [8] and [11], i.e.

$$h_i = f_5(Vc_i). \quad [12]$$

Figure 8 shows the experiment and calibration procedure. The first step of the experiment is to measure the contact probability using a needle-contact probe at several points (usually 6–9 points) between the wave top and bottom. The needle-contact probe is then removed and the voltage signal of the conductance probe is read by the data acquisition system and transferred to a personal computer. The voltage Vc_i at h_i can be calculated by the bisection method and interpolation from [11]. The voltages can be matched to film heights from [12]. From this data, a calibration curve can be obtained by a polynomial fit. Some aspects of the measurement are discussed below:

(a) As the total measuring time by the conductance probe is within a few minutes in the case of water films, the electrical conductivity and the probe status is constant within this period.
(b) In this method, it is not easy to extrapolate the correlation near the wave top ($Pn = 0$) and bottom ($Pn = 1$) in the calibration process. The measurement of probabilities by the needle-contact probe near the wave top and bottom is therefore important to enchance the reliability of the calibration.
(c) In practical measurements, this technique calibrates the total system which includes the probe, electric circuit, measuring devices etc. This enhances the repeatability and the accuracy of the measurement.
(d) The measurement of rolling or folding waves is still a formidable problem. According to Koskie *et al.* (1989), the time fraction of the folding part in a vertical water film was estimated to be <0.0001 up to the critical Reynolds number ($4\Gamma/\nu = 75{,}000$, where Γ and ν are the volume flow rate per unit width

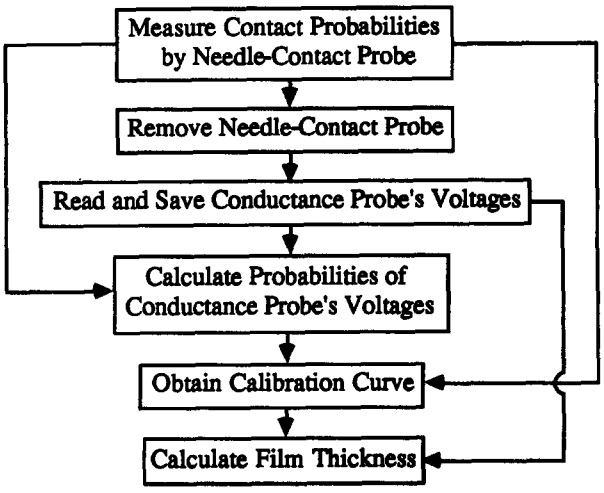

Figure 8. Calibration procedure.

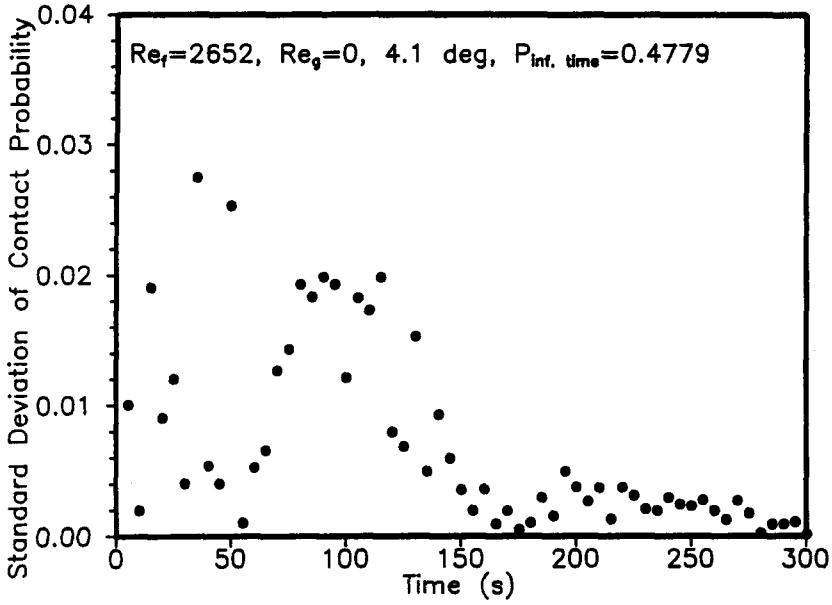

Figure 9. Contact probability variation vs measuring time.

and kinematic viscosity). In measuring water films, this method can be applied to the common range of a stratified flow.

(e) The accuracy of the contact probability measured using the needle-contact probe depends on the measuring time. For example, the variation of the contact probability for the infinite time value is within 0.5% when the measuring time is 150 s for water, as shown in figure 9.

(f) Obtaining the contact probabilities by the needle-contact probe, the contact time can be overestimated, due to the liquid holdup, especially at the moment that the liquid is separated from the needle tip after contact. This error is a function of the needle tip diameter, surface tension, viscosity of liquid and film velocity etc., but it is estimated from visual observation and the output signal that it depends greatly on the tip diameter of the needle-contact probe. A fine wire diameter of <0.075 mm greatly diminishes the liquid holdup in a water film flow. In the output signal of the needle-contact probe, the characteristic at instants of contact and separating after contact are very similar in practice. The effects of liquid holdup, therefore, are thought to be very small.

(g) When the flush-wire probe as shown in figure 1(a) is used, the wire probe attached to the translation stage can be substituted by the needle-contact probe without the need for an extra wire probe.

(h) Since the calibration technique does not directly use the conductivity of the liquid for the steady-state condition, this calibration technique can be applied to any conductance probe and also to any electrolytic liquid.

4. EXPERIMENT AND RESULTS

A schematic diagram of the experimental facility used in this study is shown in figure 10. Air is fed into the test section through the honeycomb and screen to enhance the flow quality. The water from the reservoir tank is supplied to the test section through the constant head tank and the water injection chamber. A constant water flow rate (within 1%) is maintained using a constant head tank. The water injection chamber is designed to have 25 cm of free running length to make a uniform distribution of water flow in the width direction. The water outlet of the injection chamber has dimensions of 2 cm in the flow direction by 15 cm in the width direction, on the bottom plate. The water film is initiated at the right-angled edge of the water outlet. The test section is made of transparent acrylic resin for observation by the eye. The dimensions of the test duct are

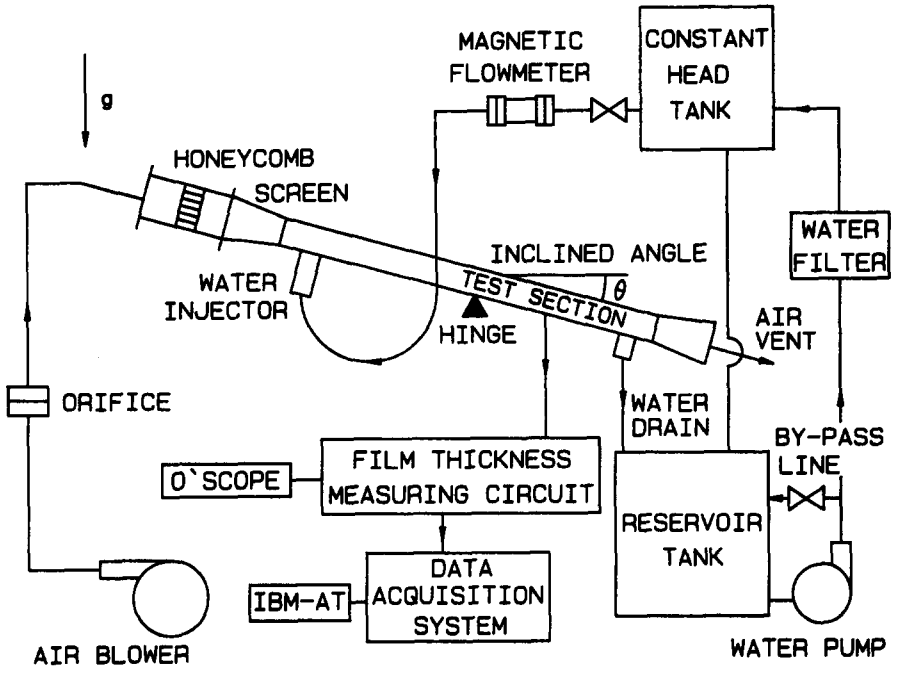

Figure 10. Schematic diagram of the experimental apparatus.

170 cm length, 15 cm width and 5.2 cm height. The inclination of the test section is changed by the hinge located at its center. The film trace is measured with three types of conductance probe at 132 cm downstream from the water inlet.

Figure 11 shows the electronic circuit used in the present study. The 100 kHz a.c. signal is applied to the flush electrode, while the signal of the wire electrode is fed into the current-to-voltage converter. This signal is then passed to a full-wave rectifier and a second-order low-pass filter set at 5 kHz. The 5 kHz cutoff allows adequate removal of the 100 kHz carrier frequency without introducing significant distortion of any signal components <1 kHz. The signal output of the low-pass filter is amplified and subtracted to increase the resolution of the data acquisition system.

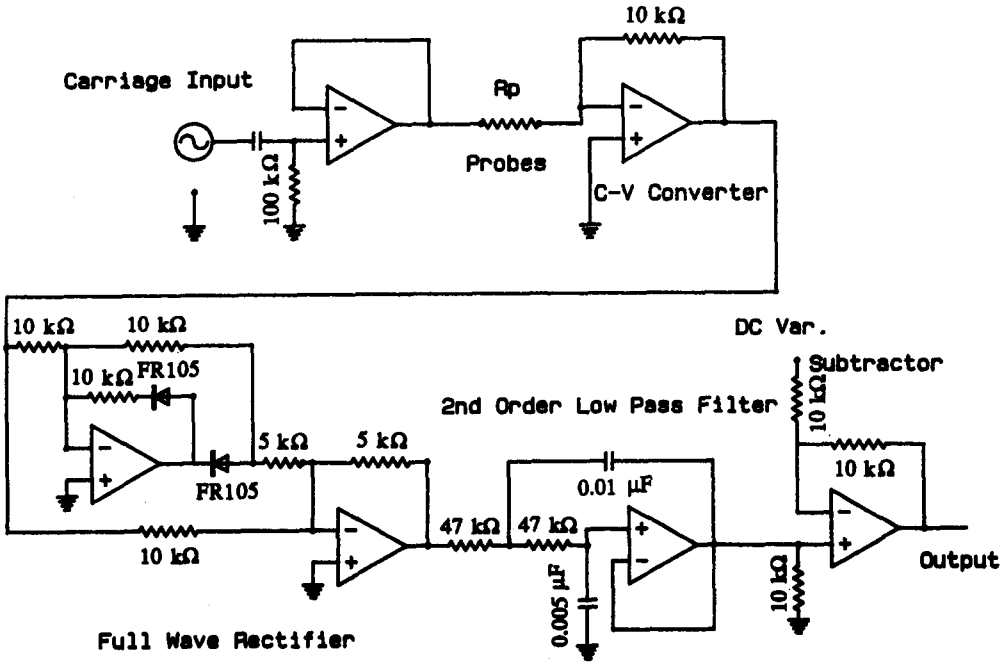

Figure 11. Electronic circuit for measuring liquid film thickness.

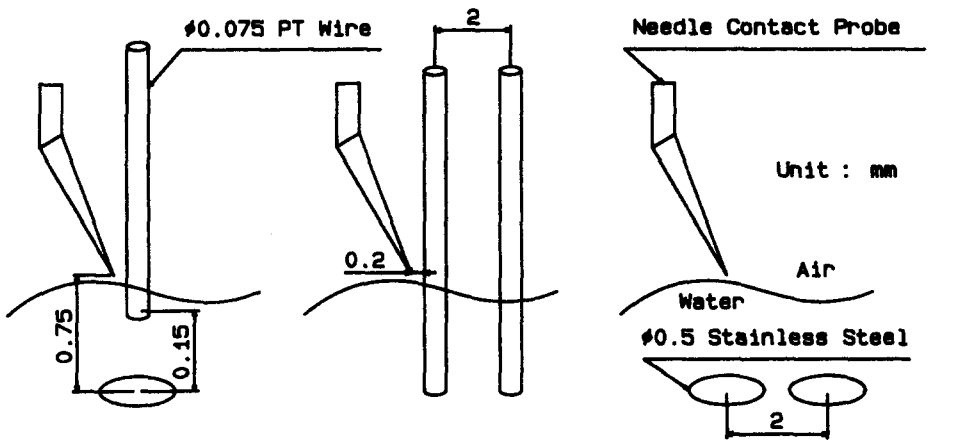

Figure 12. Experimental models of the conductance probes.

The final output is fed into the TEK 2430 digital storage oscilloscope and the Keithley Series-500 data acquisition system which has 16-bit resolution and a 33 kHz sampling rate. The wire electrode and the needle-contact probe in this experiment are attached to a micro translation stage which can be moved in 0.01 mm steps.

There is no clear technique to verify the spatial resolution of the conductance prove experimentally. The triggered signal which outputs a voltage from the conductance probe by the needle-contact probe is used to compare the spatial resolution of the three types of conductance probes discussed above. Models of parallel-wire and flush-mounted probes based on the previous research of Karapantsios *et al.* (1989) and Collier & Hewitt (1964) were constructed. Their dimensions and specifications are shown in figure 12. If the conductance probe had good repeatability and spatial resolution, the output voltages of the conductance probe at the same height would be constant. To achieve the same condition for each probe, a needle-contact probe which gives the trigger signal is located at the same elevation from the wall and 0.2 mm beside the measuring electrode. Signals from the needle-contact and conductance probes are shown in figure 13. The needle-contact probe is designed to generate only the trigger signal at the constant water level. It is made of 0.5 mm dia stainless steel wire without electrical insulation. The needle tip is sharpened to about 0.03 mm and bent to avoid crossing the probe supports, as shown in figure 12. When the water rises above the needle tip, most of the current is passed through the needle probe, since the wetted area of the needle-contact probe is far larger than that of the measuring electrode. Therefore, the signal of the conductance probe is nearly flat during the higher water level than that of the needle tip. But only the signal voltages at the point of contact, shown as solid triangles in figure 13, are used to compare the characteristics of the probe. The triggered outputs are held by the TEK 2430 digital storage oscilloscope and transferred to an IBM AT. These data are converted to heights by the calibration method described in section 3. The number of measured data is about 250 for each conductance

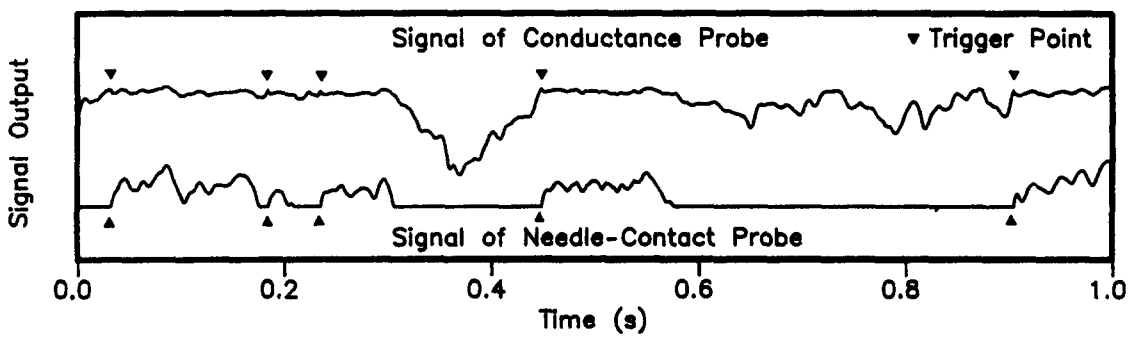

Figure 13. Triggered signals.

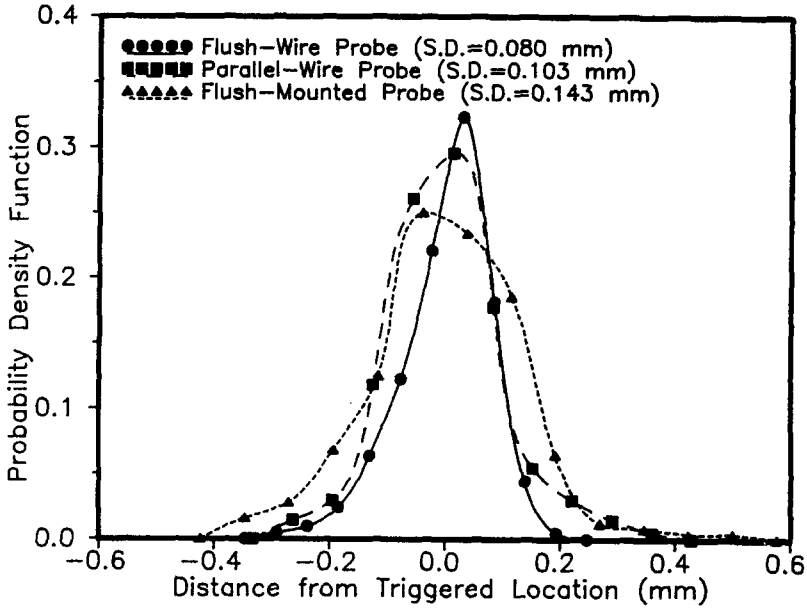

Figure 14. Distribution of triggered outputs.

probe. Figure 14 compares the probability density functions for the measurement taken by each probe at $Re_f = 2762$, $h = 0.75$ mm. The distributions show the same trends as the numerical analysis in section 2. The deviation of the flush-wire probe is smaller than that of the others, about 0.08 mm in the experimental condition. The reliability of the triggering technique using the needle-contact probe is reduced by the wave slope and the surface tension of the water etc. The average slope of the interface is estimated to be about 8° at the present experimenal range. The error due to three-dimensional waves by the 0.2 mm distance between the needle-contact probe and the measuring electrode is estimated at about 0.028 mm. Therefore, the deviation in figure 14 is due not to the triggering location but to the spatial resolution of the conductance probe.

The wire electrodes of the flush-wire and parallel-wire probes deform the interface. At low liquid flow rates, surface deformation by the wire probe is negligible, but increases with flow rate. In the same experimental condition, the contact probabilities of a needle-contact probe which is 0.2 mm from the parallel-wire and flush-wire probes are compared in figure 15. The contact probabilities

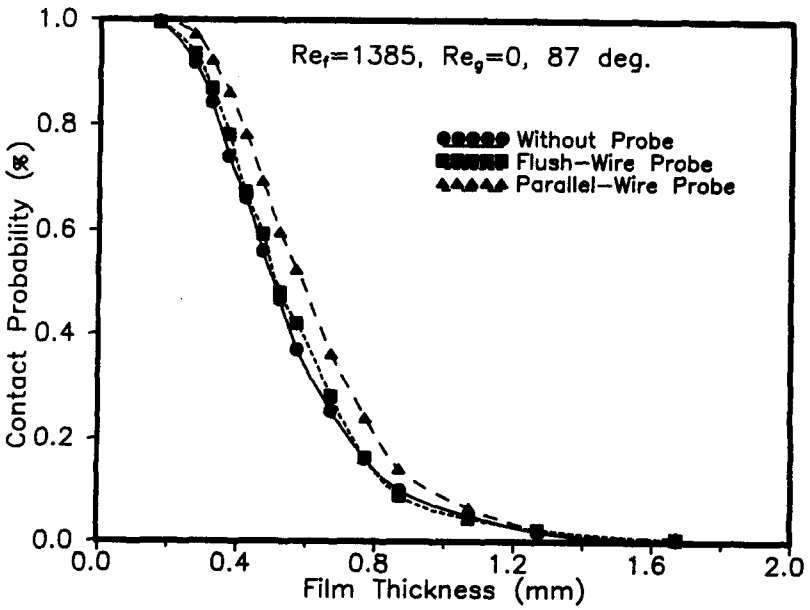

Figure 15. Interface deformation by the conductance probe.

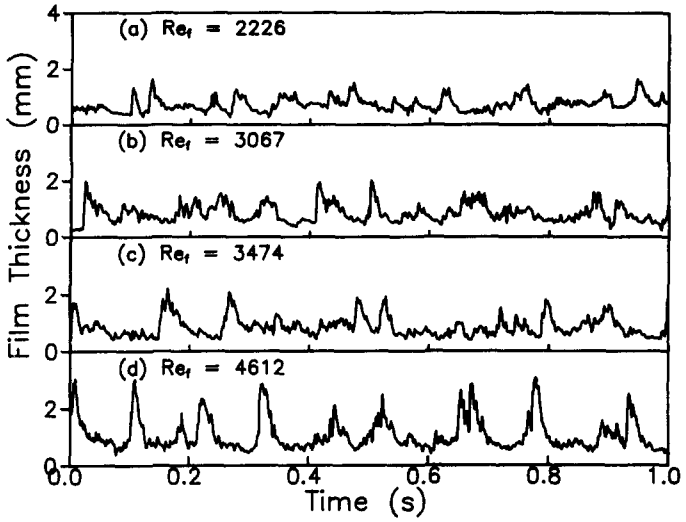

Figure 16. Typical traces of water film thicknesses.

without the wire probe are also shown. The dimensions of the flush-wire and parallel-wire probes are the same as shown in figure 12(a) and (b). The disturbance by the flush-wire probe is relatively small, while the parallel-wire probe distorts the free surface of the water by about 0.08 mm. These results show that the flush-wire probe is more reliable than the parallel-wire probe.

The wire electrode can also be deflected by wave motion created by the use of the flush-wire probe. This unacceptable condition can be avoided by optimal design of the probe. The effective length of the wire electrode is less than the wave amplitude. The minimum required length is < 5 mm in moderate stratified flow. The deflection of the wire electrode is calculated as the order of the wire diameter for a platinum wire of 0.05 mm dia or larger. When platinum is used for the electrode material, wire of small diameter is not recommended. The effect of the deflection is, however, supposed to be negligible, since the current output mainly depends on the depth of the immersed length of the wire electrode.

With the flush-wire probe shown in figure 12(a) and the calibration technique presented in section 3, the instantaneous film thicknesses are measured. The liquid film thickness traces along the time at various film Reynolds numbers are shown in figure 16. The global shapes in figure 16 are similar to the results obtained by Chu & Dukler (1975) and Koskie *et al.* (1989). The film thickness data of Chu & Dukler, who used the flush-mounted probe, showed that the thick film was smoothened. The data of Koskie *et al.*, who used the parallel-wire probe, showed that the thin

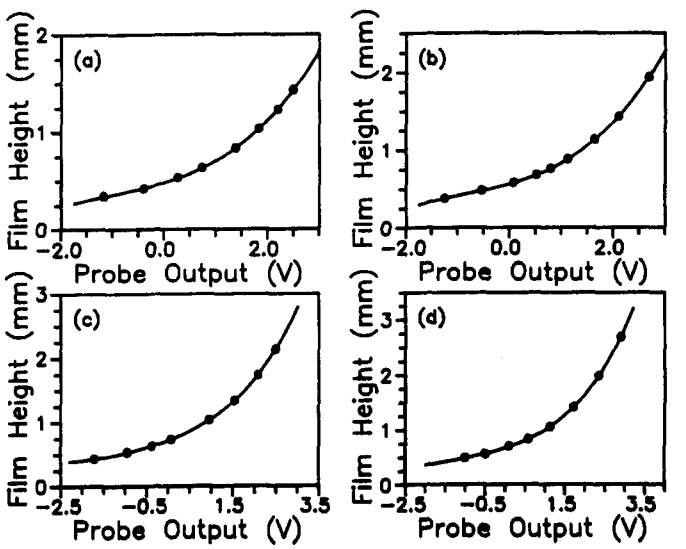

Figure 17. Calibration curves for figure 16.

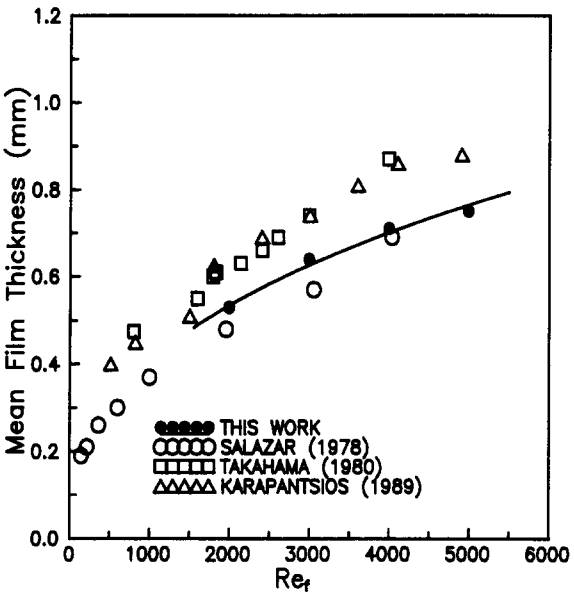

Figure 18. Comparison of mean film thickness in a vertical free-falling film.

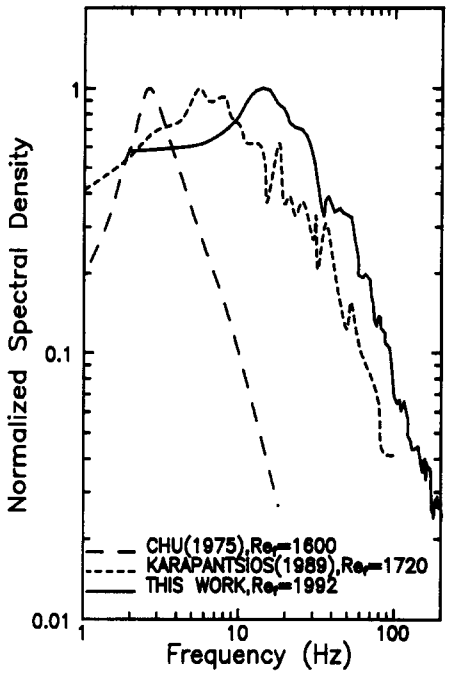

Figure 19. Comparison of the normalized spectral density function of film thickness in a vertical free-falling film.

film trace was flattened. The thicknesses of the base film in figure 16 is, however, measured to be thicker than the results of Koskie *et al.*, who mentioned that their result for the base film thickness might have some discrepancies from that of the needle-contact probe. The film trace variations of this experiment in figure 16 range from 0.3 to 3 mm film thickness.

Figure 17 shows calibration graphs corresponding to each case in figure 16. The calibration curves are obtained using a fourth-order polynomial fit. The measured points are well-matched to the calibration curves for all of the experimental conditions.

The mean film thickness measured by the flush-wire probe is compared with other work in figure 18 for a vertical air–water stratified flow. The experimental conditions such as test geometry, inclined angle, the measuring location from the inlet and the measuring method are described in table 1. The inclined angle and the measuring location are slightly different from other experiments, but these are not supposed to be the dominant factors for this comparison. The mean film thickness in this work is about 0.1 mm lower than those of Takahama & Kato (1980) and Karapantsios *et al.* (1989), but slightly larger than that of Salazar & Marschall (1978). Takahama & Karapantsios's result, the water film thickness inside a pipe, might be larger than that on a flat plate because of the curvature effect. The film thickness of the present work is closer to Salazar's results, which used the laser scattering method without an electrode. The mean film thickness results generally agree with those of previous experiments.

The flush-wire probe can detect the interface shape without losing the small waves, since it has fine spatial resolution. The good spatial resolution gives, finally, better temporal resolution when the film thickness is measured at the fixed point. In figure 19, the spectral density of film thickness measured by the flush-mounted probe is compared with those of Chu & Dukler (1974) and Karapantsios *et al.* (1989) in a vertical stratified flow at a similar film Reynolds number ($Re_f = 1600$–1992). The spectral density functions are normalized by their maximum values. In data analysis of this work, the Hanning window function is applied to obtain the spectral density function by the same procedure as Karapantsios *et al.* The flush-mounted probe used by Chu & Dukler diminishes the high frequency signal more than the parallel-wire probe used by Karapantsios *et al.* The flush-wire probe in this work, however, detects a higher range of wave frequency than the previous method. The modal frequency in this work is about 15 Hz, which

Table 1. Experimental conditions to compare the experimental data in a vertical stratified flow without air flow

Research	Geometry	Inclined angle (deg)	Measuring location (m)	Measuring method
This work	Flat plate	87	1.32	Flush-wire probe
Chu & Dukler (1975)	Pipe inside	90	1.83–3.97	Flush-mounted probe
Salazar & Marschall (1978)	Flat plate	90	1.34	Laser scattering
Takahama & Kato (1980)	Pipe inside	90	1.32	Needle & capacitance probe
Karapantsios *et al.* (1989)	Pipe inside	90	2.5	Parallel-wire probe

Karapantsios *et al.* referred to as the second peak of the spectral density, and far larger than that of the other experiment. The high-frequency component of the liquid film, the small waves, was underestimated in the previous work. The differences between the experimental data can depend on the experimental conditions and apparatus, but the main reason is believed to be the measuring method and probe types. The spatial resolution is shown to be very important for the understanding of dynamic behavior such as film velocities, film wave frequency etc. This film thickness measuring technique will be used in measuring three-dimensional wave traces, modeling interfacial structure and clarifying wave phenomena.

5. CONCLUSIONS

The newly developed flush-wire probe used in the measurement of liquid film thicknesses enhances spatial resolution. For a large flush electrode diameter and the proper immersed length ratio, the flush-wire probe gives up to 0.1 mm of spatial resolution. This conductance probe is easier to set up and handle than the previous types of conductance probes. A new calibration method using the probability of existence of the liquid at a constant flow rate is also presented. This technique is more stable, accurate and repeatable than traditional calibration techniques. Moreover, it can be applied to any type of conductance probe and any fluid for wide ranges of liquid film heights.

Acknowledgements—This work was performed with the support of the Korea Science & Engineering Foundation and the Research Institute of Science and Technology. The authors are grateful for this financial support.

REFERENCES

AKAI, M., INOUE, A., AKOKI, S. & ENDO, K. 1980 Structure of a cocurrent stratified two-phase flow with wavy interface. *Int. J. Multiphase Flow*, **6**, 173–190.

BROWN, R. C., ANDREUSSI, P. & ZANELLI, S. 1978 The use of wire probes for measurement of liquid film thickness in annular gas–liquid flows. *Can. J. Chem.* **56**, 754–757.

CHU, K. J. & DUKLER, A. E. 1974 Statistical characterstics of thin, wavy films: part II. Studies of the substrate and its wave structure. *AIChE Jl* **20**, 695–706.

CHU, K. L. & DUKLER, A. E. 1975 Statistical characteristics of thin, wavy films: part III. Structure of the large waves and their resistance to gas flow. *AIChE Jl* **21**, 583–593.

COLLIER, J. G. & HEWITT, G. F. 1964 Film thickness measurement. ASME Paper 64-WA/HT-41.

CONEY, M. W. E. 1973 The theory and application of conductance probes for the measurement of liquid film thickness in two-phase flows. *J. Phys. E: Scient. Instrum.* **6**, 903–910.

GOLDSTEIN, R. J. 1983 *Fluid Mechanics Measurements*, pp. 479–498. Hemisphere, Washington, DC.

KARAPANTSIOS, T. D., PARAS, S. D. & KARABELAS, A. J. 1989 Statistical characteristics of free falling films at high Reynolds numbers. *Int. J. Multiphase Flow* **15**, 1–21.

KOSKIE, J. E., MUDAWAR, I. & TIEDERMAN, W. G. 1989 Parallel-wire probes for measurement of thick liquid films. *Int. J. Multiphase Flow* **15**, 521–530.

MIYA, M., WOODMANSEE, D. E. & HANRATTY, T. J. 1971 A model of roll waves in gas–liquid flow. *Chem. Engng Sci.* **26,** 1915–1931.

NEAL, L. G. & BANKOFF, S. G. 1963 A high resolution resistivity probe for determination of local void properties in gas–liquid flow. *AIChE Jl* **9,** 490.

SALAZAR, R. P. & MARSCHALL, E. 1978 Time average local thickness measurement in falling liquid film flow. *Int. J. Multiphase Flow.* **4,** 408–412.

SOLOMON, V. J. 1962 Construction of a two-phase flow regime transition detector. M.S. Thesis, Mech. Engng Dept, MIT, Cambridge, MA.

SWANSON, R. W. 1966 Characteristics of the gas–liquid interface in two phase annular flow. Ph.D. Thesis, Univ. of Delaware, Newark, DE.

TAKAHAMA, H. & KATO, S. 1980 Longitudinal flow characteristics of vertically falling liquid films without concurrent gas flow. *Int. J. Multiphase Flow.* **6,** 203–215.